Theoretical Prediction of Electric Field-Enhanced Coalescence of Spherical Drops

Xiaoguang Zhang
Chemical Technology Div., Oak Ridge National Laboratory, Oak Ridge, TN 37831
Dept. of Chemical Engineering, University of Tennessee, Knoxville, TN 37996

Osman A. Basaran and Robert M. Wham
Chemical Technology Div., Oak Ridge National Laboratory, Oak Ridge, TN 37831

A fundamental study of drop collision, coalescence and growth induced by combined effects of gravitational and electrostatic forces is presented. The focus is on the enhancement of rates of collision and growth of spherical, conducting drops bearing zero net charge in dilute, homogeneous dispersions by an external electric field. By completely accounting for hydrodynamic and electrostatic interactions, a trajectory analysis is used to follow the relative motion of two drops and predict pairwise collision and coalescence rates. A population dynamics equation is then solved to predict the evolution in time of the size distribution and the average size of drops. The results show that the rates of drop collision and growth can be increased significantly by applying an electric field, in accord with fundamental experiments and patents on electrocoalescence. The enhancement of drop collision and coalescence is especially pronounced when the imposed electric field acts horizontally, that is, in a direction perpendicular to gravity.

Introduction

Enhancement of coalescence of drops by electric fields is of importance in many technological applications, such as phase separations (Ptasinski and Kerkhof, 1992), and prevalent in natural phenomena, such as raindrop growth (Sartor, 1969). Unfortunately, in spite of the relative widespread use of electric fields as a means of improving drop coalescence, as reviewed by Waterman (1965) and Ptasinski and Kerkhof (1992), a complete fundamental understanding and comprehensive prediction of the enhancement of coalescence of drops by an electric field is lacking because of the complexity of electrostatic and hydrodynamic interactions among swarms of drops dispersed in a fluid. A goal of this work is to remedy this situation by accounting for the effects of electric-field-induced forces and hydrodynamic interactions on drop coalescence from first principles when the drops—the dispersed phase—are conducting and the fluid surrounding them—the continuous phase—is insulating.

In a variety of processes involving dispersions of small drops of one fluid in a second, immiscible fluid, the drops undergo relative motion due to different driving forces, which results in their possible collisions and coalescence. As a result of drop coalescence, the average drop size in a dispersion increases and its size distribution shifts toward the larger size over time from its initial distribution. In a quiescent fluid on earth, driving forces that cause dispersed drops to migrate relative to each other include gravitational force and electrostatic forces arising from charges induced by an imposed electric field, among others. Under the action of gravity, the settling velocity of an isolated drop at low Reynolds number is proportional to the square of its radius (Hadamard, 1911; Rybczynski, 1911). Thus, the larger drops settle more rapidly than and catch up to the smaller drops in their path, leading to possible collision and coalescence. Application of an external electric field, no matter how small, induces charges of the opposite sign on the closest sides of two conducting drops (Davis, 1964). Attraction between the induced charges of the opposite sign on the two nearby drops causes them to approach each other rapidly and increases the possibility of their collision and coalescence. When two drops are within several radii of each other, the presence of the neighboring drop disturbs the velocity field around each drop. These disturbances

Correspondence concerning this article should be addressed to O. A. Basaran.

bring about an additional hydrodynamic resistance on each drop, and cause the drops to flow around each other. If two drops are sufficiently close, van der Waals attraction may also become important: this force can help to pull nearby drops into contact and literally hold them together during coalescence. When the drops come into physical contact, they coalesce into a single, large drop due to the tendency of interfacial tension to minimize the surface area and energy of the drops in contact.

In this article, we present theoretical work to predict the rate of pairwise drop collision induced by combined effects of gravity and electric-field-induced forces employing a trajectory analysis. We thereby determine the resultant shift in the drop size distribution and increase in the average drop size by using the pairwise coalescence rate in a population dynamics model. Of particular interest is to quantify the enhancement of drop coalescence by an externally applied electric field. Attention is restricted in this article to conducting drops that bear zero net charge, are free from adsorbed surfactants, and are surrounded by a linearly polarizable dielectric fluid or insulator (Landau and Lifshitz, 1960). The drops are assumed to be sufficiently small—typically having diameters of a few hundred microns, or less—and the strength of the applied electric field is taken to be on the order of a few kilovolts per centimeter or less, that they remain spherical under the action of interfacial tension forces, and that inertial forces are negligible compared to viscous ones (Latham and Roxburgh, 1966; Zhang and Davis, 1991). However, the drops are large enough—typically having diameters of a few microns, or more—so that Brownian diffusion is negligible (Zhang and Davis, 1992). Moreover, both the drop and the continuous phases are taken to be Newtonian fluids with constant physical properties.

As two drops approach one another, the strength of the electric field in the region between their points of closest separation can attain values many times that of the imposed or applied electric field far from the drops, a result of the mutual interactions between the induced charges on the drop surfaces. A general solution, based on separation of variables in bispherical coordinates, has been developed by Davis (1964) that determines the variation of the disturbed electric field everywhere outside and the charges induced on the surfaces of two different-sized conducting drops under an arbitrary electric field. The method of separation of variables used to solve the Laplace equation that governs the electric potential field outside the drops yields series expressions for the strength of the local electric field and the electrostatic force between two drops. The solution diverges when the distance between the two drops tends to zero, indicating a dramatic increase in the strength of the electric field. The increase in the strength of the electric field between two drops with decreasing separation between them has been confirmed experimentally by Latham and Roxburgh (1966) for the axisymmetric problem of two identical conducting drops immersed in an insulating fluid where the line joining their centers lies along the direction of the imposed electric field.

The increased strength of the local electric field enhances the electrostatic force of attraction between two nearby drops and speeds the rate of approach of the drops. When the drops are within a critical distance of one another, the fluid film separating them can rupture rapidly, followed by the coalescence of the drops. This is either because the electric field between the two drops has attained the dielectric breakdown strength of the surrounding fluid (Allan and Mason, 1962), or the fluid film has succumbed to an electrohydrodynamic instability (Michael and O'Neill, 1970).

Enhanced coalescence of conducting drops in an external electric field has been investigated theoretically and experimentally by Williams and Bailey (1983, 1986). In making their theoretical predictions on the effects of electric fields on drop coalescence, however, they used an approximate solution for electric-field-induced forces, which is not valid when two drops are close to one another. Moreover, they did not account for hydrodynamic interactions between the two drops in their studies, which results in a considerable overestimation of the coalescence rate (cf. Zhang and Davis, 1991, and see what follows).

Effects of hydrodynamic interactions between two drops undergoing relative motion under conditions of Stokes flow have been completely studied by Kim and Karrila (1991), Haber et al. (1973), and Zinchenko (1981), among others, for motions along and normal to the line joining the centers of the two drops. The hydrodynamic resistance opposing the relative motion of two spheres is found to increase as the viscosity of the drop fluid increases and depends on the geometry of the two spheres. In particular, for motion along the line of centers of the two spheres, the resistance varies with their relative positions as $1/f(h)$, where h is the closest distance between the surfaces of the spheres and $f(h)$ stands for h, $h^{1/2}$, and $\ln h$ when the two spheres are rigid particles, liquid drops, and bubbles, respectively. Effects of hydrodynamic interactions on drop collision and coalescence have been rigorously investigated recently for drop motion driven by Brownian diffusion (Zhang and Davis, 1991), gravity (Zhang and Davis, 1991), and interfacial tension gradients (Zhang and Davis, 1992; Satrape, 1992), acting independently. These studies have shown that hydrodynamic interactions reduce collision and coalescence rates significantly, particularly for gravity-induced collisions.

This work employs solutions developed earlier for the hydrodynamic interactions and electric-field-induced attractions between two spherical, conducting drops and calculates electric-field-enhanced collision and coalescence rates based on a trajectory analysis. Moreover, the determined pairwise coalescence rates are subsequently used in a population dynamics model (Berry and Reinhardt, 1974) to predict the evolution of a population of drops in a dilute, homogeneous dispersion. The theoretical development and predictions of the pairwise collision rates induced by the combined effects of gravitational and electrostatic forces are detailed. Most results of this article are presented in dimensionless form, except for illustrative purposes of the enhancement of drop collision and growth in a typical dilute, homogeneous water–oil dispersion.

Theory

The analysis is restricted to binary interactions and coalescence in a dilute, homogeneous suspension of conducting, spherical drops of viscosity μ_d and density ρ_d dispersed in an immiscible fluid of viscosity μ_0, density ρ_0, and relative permittivity, or dielectric constant, ϵ. It is further taken that

changes in drop sizes are caused only by drop coalescence with drop dissolution, diffusion or Ostwald ripening, or breakup being negligible over the time scale of coalescence.

To predict the temporal evolution of the drop-size distribution during a phase-separation process, a distribution of drop sizes is divided, or discretized, into n discrete categories that have equal spacing in the logarithm of drop mass or volume. The resulting population dynamics equation that describes the evolution of this distribution due to drop coalescence is provided by a mass conservation balance on each size category, i (Rogers and Davis, 1990):

$$\frac{dn_i}{dt} = \frac{1}{2}\sum_{j=1}^{i-1} J_{i-j,j} - \sum_{j=1}^{n} J_{ij}, \tag{1}$$

where n_i is the number of drops of size i per unit volume, t is time, and J_{ij} is the rate of collision per unit volume of drops of size i with drops of size j. The first term on the right side of Eq. 1 is the rate of formation of drops of size i by collisions of two smaller drops (the factor of 1/2 is to avoid double counting), and the second term is the rate of loss of drops of size i due to their collisions to form larger drops.

The collision rate appearing in Eq. 1 may be expressed as (Zhang and Davis, 1991)

$$J_{ij} = n_i n_j \pi (a_i + a_j)^2 \, |\underline{U}_i^{(0)} - \underline{U}_j^{(0)}| \, e_{ij}, \tag{2}$$

where a_i is the characteristic radius of size category i, $\underline{U}_i^{(0)}$ is the average velocity of drops of size i due to gravity only, and e_{ij} denotes the collision efficiency that is defined as a ratio of the actual collision rate to that for rectilinear drop motion due to gravity alone in the absence of interactions between drops. Differing from unity, the collision efficiency describes effects of electric-field-induced forces, van der Waals attraction, and hydrodynamic interactions on drop collision and coalescence.

Relative motion of two spherical, conducting drops

For binary interactions of drops with radii a_i and a_j undergoing small Reynolds number flow, as sketched in Figure 1, the external driving forces on each drop balance the hydrodynamic resistance, and the velocity, $\underline{V}_{ij} = \underline{U}_i - \underline{U}_j$ of drop i relative to drop j is linearly related to the sum of the external forces and depends only on the instantaneous relative position of the two drops (Batchelor, 1982). Moreover, the relative velocity can be decomposed into two components, one for motion along and another for motion normal to the line-of-centers:

$$\underline{V}_{ij} = V_{ij}^{(0)}(-L\cos\theta \underline{e}_r + M\sin\theta \underline{e}_\theta) - \frac{D_{ij}^{(0)}}{kT}\left(GF_{E,ij}^{r}\underline{e}_r - HF_{E,ij}^{\theta}\underline{e}_\theta\right) - \frac{D_{ij}^{(0)}}{kT}GF_{V,ij}\underline{e}_r, \tag{3}$$

where $\underline{e}_r$ and $\underline{e}_\theta$ are unit vectors in the radial and tangential directions in a spherical polar coordinate system shown in Figure 1, k is Boltzmann's constant, and T is the absolute temperature. The three terms on the right side of Eq. 3 represent contributions of gravitational forces, electric-field-induced forces, and van der Waals attraction, respectively, on the relative motion of two drops. The relative velocity of two widely separated drops due to gravity is given by the Hadamard–Rybczynski formula (Hadamard, 1911; Rybczynski, 1911):

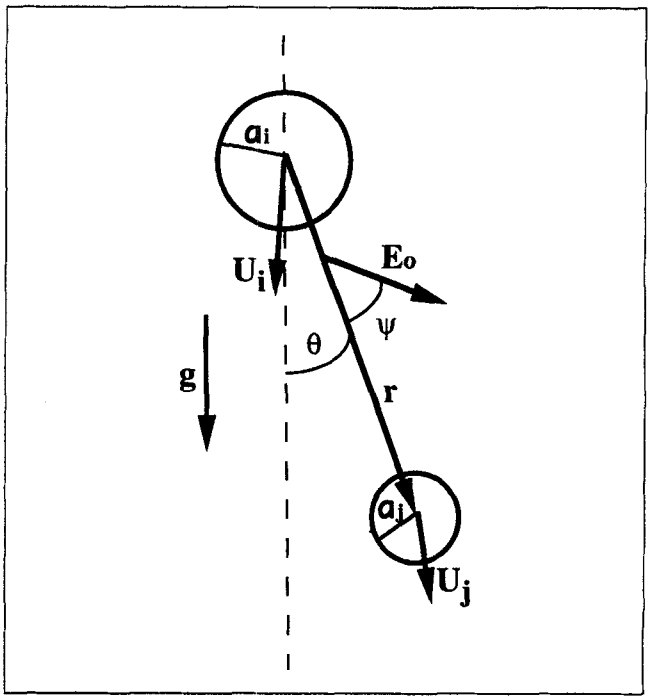

Figure 1. Coordinate system used for the relative motion of two different-sized drops induced by gravity and electrostatic forces.

$$V_{ij}^{(0)} \equiv |\underline{U}_i^{(0)} - \underline{U}_j^{(0)}| = \frac{2(\hat{\mu}+1)\,|\rho_d - \rho_0|\,a_i^2(1-\lambda^2)g}{3(3\hat{\mu}+2)\mu_0}, \tag{4}$$

where $\hat{\mu} = \mu_d/\mu_0$ is the viscosity ratio, $\lambda = a_j/a_i$ is the ratio of the radius of the small drop to that of the large drop, and g is the magnitude of the gravitational acceleration vector. The relative mobility of two widely spaced drops due to an equal and opposite force, such as the electric-field-induced force and van der Waals attraction, is

$$D_{ij}^{(0)} = \frac{kT(\hat{\mu}+1)(1+\lambda)}{2\pi u_0(3\hat{\mu}+2)a_i\lambda}. \tag{5}$$

The van der Waals force, $F_{V,ij}$, is generally important only when the drops are very close together and acts along their line-of-centers. It is commonly expressed as the gradient of its potential, namely, $F_{V,ij} = \nabla\Phi_{ij}$ (Hamaker, 1937):

$$\Phi_{ij} = \frac{A}{6}\left\{\frac{8\lambda}{(s^2-4)(1+\lambda)^2} + \frac{8\lambda}{s^2(1+\lambda)-4(1-\lambda)^2} + \ln\left[\frac{(s^2-4)(1+\lambda)^2}{s^2(1+\lambda)^2-4(1-\lambda)^2}\right]\right\}, \tag{6}$$

where A is the composite Hamaker constant and $s = 2r/(a_i + a_j)$ is the dimensionless distance between two drop centers, with r denoting the dimensional distance between the two drop centers.

Electric-field-induced forces on two conducting drops are determined by solving for the distribution of electric field around the drops by means of a bispherical coordinate method (Davis, 1964). The forces are decomposed into two components, along and normal to the line-of-centers of the drops, $F^r_{E,ij}$ and $F^\theta_{E,ij}$, respectively:

$$F^r_{E,ij} = 4\pi\epsilon a_j^2 E_0^2 (F_1 \cos^2\psi + F_2 \sin^2\psi), \quad (7)$$

$$F^\theta_{E,ij} = 4\pi\epsilon a_j^2 E_0^2 F_3 \sin 2\psi, \quad (8)$$

where E_0 is magnitude of the externally applied electric field that is approached infinitely far from the two drops, and ψ is the angle that the applied electric field makes with the vector joining the line-of-centers of the two drops, as shown in Figure 1. The force coefficients, F_i ($i = 1$, 2, and 3), are complicated series expressions that depend on the relative geometry of the two drops (on λ and s). These coefficients and hence the electrostatic forces are determined numerically using the solution of Davis (1964). In order to achieve convergence of the solution for drops in near-contact, a large number of terms in the series is calculated with a convergence criterion of $|S_{n+1} - S_n|/S_n \leq 1 \times 10^{-7}$, where S_n is the nth partial sum of the series. For a given electric field, the induced electrostatic force between two conducting drops is known approximately to be inversely proportional to the fourth power of drop separation (Waterman, 1965). Therefore, like the van der Waals force, the electric-field-induced force increases dramatically with decreasing separation between two drops and becomes an important factor in causing two drops to approach each other only when the two drops are close to one another. In contrast to the van der Waals force, the electric-field-induced force increases as the square of the drop size, which implies that this force would have a relatively larger effect on large drops. These features are quantitatively shown in Figure 2 where the electric-field-induced force, nondimensionalized by $4\pi\epsilon[(a_i + a_j)/2]^2 E_0^2$, on two drops along their line-of-centers, $\hat{F}^r_{E,ij}$, is plotted as a function of drop separation for different size ratios and $\psi = 0$. The dimensionless van der Waals force, scaled by $2A/(a_i + a_j)$, $\hat{F}_{V,ij}$, is also presented in this figure for comparison. The van der Waals force is seen to act over a rather short range of drop separations, and hence is expected to play a role in pulling together two approaching drops only when they are in close proximity of one another, as compared to the electric-field-induced force. It is noteworthy, however, that since the electric-field-induced force increases with increasing drop size, it may dominate over the van der Waals force in causing the coalescence of large drops.

The magnitude and direction of the electric-field-induced force between two drops vary with the orientation of the external electric field relative to the line-of-centers of the two drops, as qualitatively depicted in Figure 3. Figures 4 and 5 show the variation of the dimensionless electric-field-induced forces along and normal to the line-of-centers, $\hat{F}^r_{E,ij}$ and $\hat{F}^\theta_{E,ij}$, respectively, with the orientation of the electric field or, in other words, with the angle ψ between the electric field and

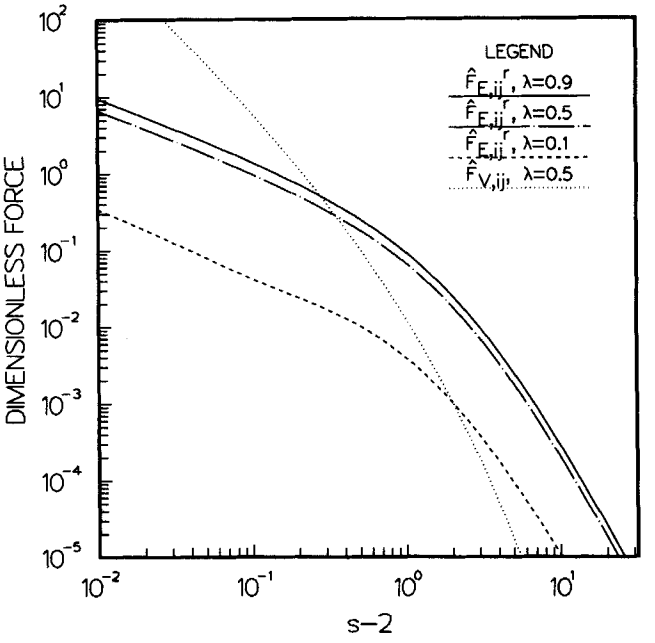

Figure 2. Dimensionless electric-field-induced and van der Waals forces along the line of centers of two drops as a function of the dimensionless distance between drop surfaces for $\psi = 0$ and different size ratios.

the line joining the centers of the two drops at different separations. Figure 4 shows that the force along the line of centers attains a maximum when $\psi = 0$ and decreases monotonically with increasing ψ (cf. Figures 3a and 3b). Most important, Figure 4 shows that the electric force along the line of centers becomes repulsive, $\hat{F}^r_{E,ij} < 0$, as ψ approaches $\pi/2$ (see the insert to Figure 4), a result having practical implications. Figure 3c makes plain that this repulsion occurs because when $\psi \sim \pi/2$ the induced charges on the near sides of the two drop surfaces are distributed in such a fashion that repulsion between charges of the same sign on the two drops is stronger than attraction between charges of the opposite sign due to

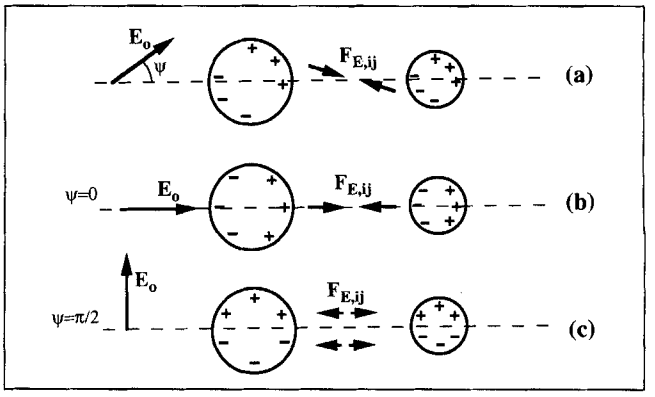

Figure 3. Surface densities of charge and forces on two drops induced by an externally applied electric field for different values of angle ψ between the electric field and the line joining centers of the two drops (cf. Figure 1).

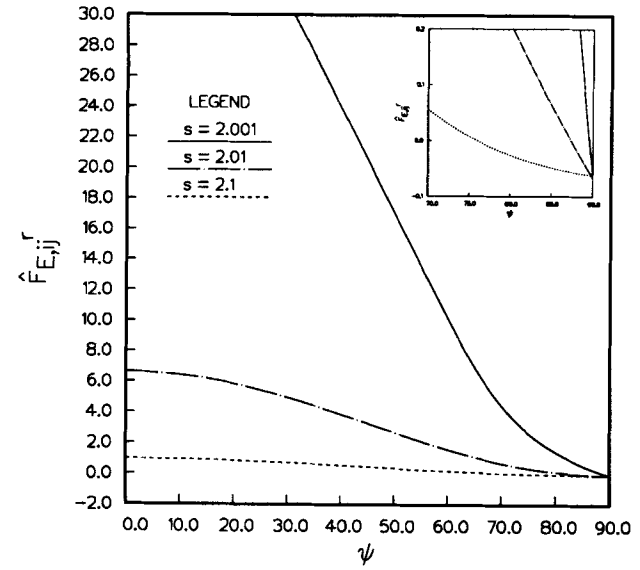

Figure 4. Dimensionless electric-field-induced force along the line of centers as a function of the angle ψ between the electric field and the line joining centers of two drops for different separations of the two drops.

Insert: A blowup that shows the variation of the electric-field-induced force near $\psi \sim \pi/2$.

the Coulombic nature of the interaction between surface charges (Landau and Lifshitz, 1960). Moreover, this repulsion, although of small magnitude, leads to a considerable difference in the nature of drop collision and coalescence under differently oriented electric fields, a point that is discussed in detail later on in this article. With this important discovery, the present model provides useful guidance for optimum orientation of an electric field to promote drop collision and coalescence in experiments and practical applications. Figure 5 shows that the electric-field-induced force normal to the line of centers is much weaker than that along the line of centers and vanishes as the angle ψ tends to 0 or $\pi/2$, as plainly indicated by Eq. 8 and implied in Figure 3.

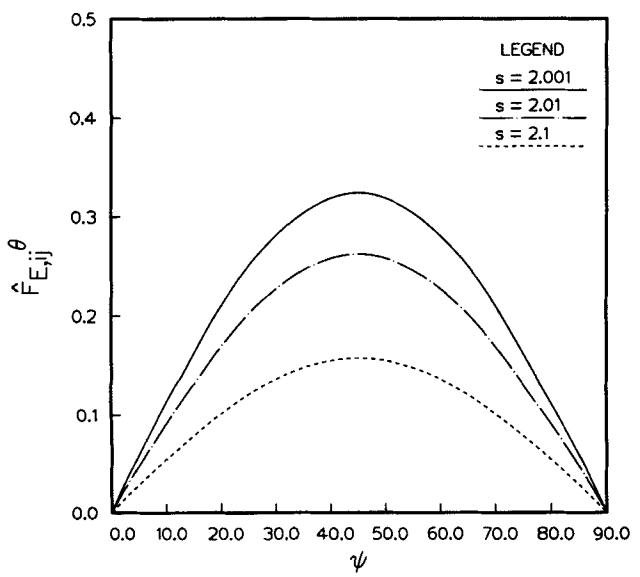

Figure 5. Dimensionless electric-field-induced force normal to the line of centers as a function of the angle ψ between the electric field and the line joining centers of two drops for different separations of the two drops.

The relative mobility functions in Eq. 3 for motion along the line of centers, L and G, and motion normal to the line of centers, M and H, are used to conveniently describe the effects of hydrodynamic interactions between two drops (Batchelor, 1982). These functions depend on the size ratio of two drops, λ, the viscosity ratio, $\hat{\mu}$, and the dimensionless distance between two drops, s. Several analytical solutions for the mobility functions are available and analytical expressions and numerical values of these functions for arbitrary values of λ, $\hat{\mu}$, and s have been collected and presented by Zhang and Davis (1991). In this article, the complete solutions for the hydrodynamic interactions are obtained using the bispherical coordinate method to solve for the velocity fields inside and outside the drops (Haber et al., 1973; Zinchenko, 1981). The relative mobility functions approach unity when the drops are widely separated indicating the decay of hydrodyamic interactions. As the drops approach each other, the mobility functions decrease due to increasing strength of these interactions, resulting in a significant resistance to the relative motion and collision of the two drops. Moreover, the effects of hydrodynamic interactions become more important as the viscosity ratio increases. It is noteworthy that the hydrodynamic interaction force decays slowly as the distance separating the two drops increases, and therefore possesses longer range effects on the relative motion of two drops compared to those due to electric-field-induced forces or van der Waals attraction. Thus, two widely separated drops may not be brought into collision and coalescence under electric-field-induced forced alone, unless other long-range forces (such as gravity) are present to cause the drops to get sufficiently close to one another for the electric-field-induced forces to be important.

Trajectory analysis for the collision rate of two drops

For a specified system, the collision rate is readily determined via Eq. 2, except for the collision efficiency, e_{ij}, which describes the effects of hydrodynamic interactions, electric-field-induced forces, and van der Waals forces on collision and coalescence of two drops and depends on the relative importance of these effects. The collision efficiency is determined by a trajectory analysis, which is based on a force balance as shown in Eq. 3 (Tien and Payatakes, 1979). Starting from appropriate initial conditions, drop trajectories can be obtained by integrating the force balance Eq. 3. When drop inertia is negligible as in this article, the drop trajectories do not cross one another: therefore, a limiting trajectory can be determined along which two drops approach each other with the largest possible horizontal displacement, y_c, from the vertical axis of symmetry such that they eventually will just collide, as shown in Figure 6. Any relative trajectories that are inside this limiting trajectory end with the drops colliding, whereas those outside the limiting trajectory end with the drops separating. Comparing the limiting trajectory with the rectilinear approach up to the instant of contact of two non-

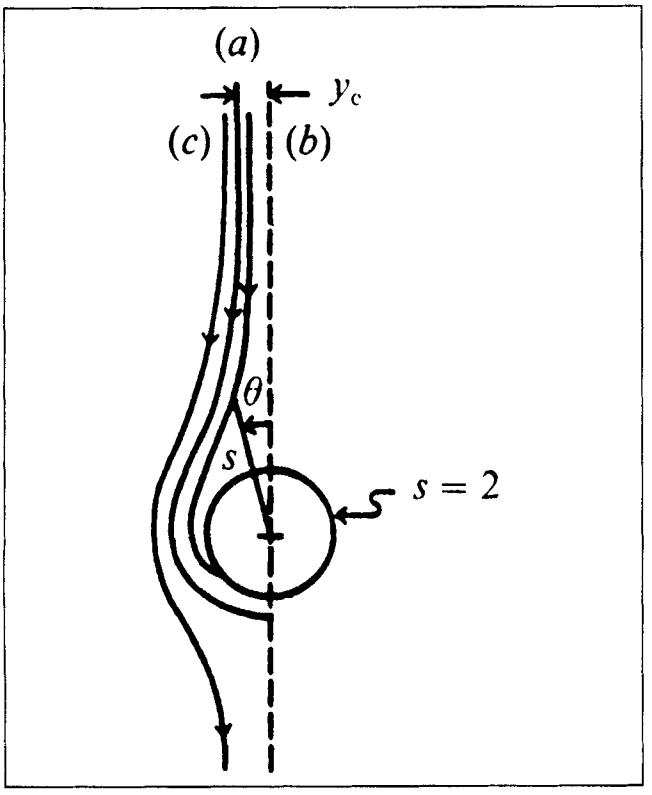

Figure 6. Possible relative trajectories of two drops: (a) the limiting trajectory; (b) a trajectory terminating with contact; and (c) a trajectory for which two drops move past one another and separate.

interacting drops under gravity only, the effects of the electric-field-induced forces, van der Waals forces, and hydrodynamic resistances, or the collision efficiency, e_{ij}, can be determined by (Zhang and Davis, 1991):

$$e_{ij} = \frac{y_c^2}{(a_i + a_j)^2}. \tag{9}$$

Thus, the determination of the collision efficiency, or the collision rate, is reduced to one of determining the critical impact displacement, y_c, of the limiting trajectory.

Nondimensionalizing the relative velocity (Eq. 3) with $V_{ij}^{(0)}$ and dividing the radial component by the tangential component yields the needed trajectory equation:

$$\frac{ds}{d\theta} = s\frac{-L\cos\theta - \dfrac{G}{Q_{E,ij}}\left(\dfrac{2\lambda}{1+\lambda}\right)^2(F_1\cos^2\psi + F_2\sin^2\psi) - \dfrac{G}{Q_{V,ij}}\dfrac{a_i+a_j}{2}\nabla\left(\dfrac{\Phi_{ij}}{A}\right)}{M\sin\theta + \dfrac{H}{Q_{E,ij}}\left(\dfrac{2\lambda}{1+\lambda}\right)^2 F_3\sin 2\psi}, \tag{10}$$

where $Q_{E,ij}$ and $Q_{V,ij}$ are parameters that represent the relative importance of gravitational forces to electric field-induced forces and van der Waals forces, respectively:

$$Q_{E,ij} \equiv \frac{V_{ij}^{(0)}}{\dfrac{D_{ij}^{(0)}}{kT}4\pi\epsilon\left(\dfrac{a_i+a_j}{2}\right)^2 E_0^2} = \frac{4|\rho_d - \rho_o|\lambda(1-\lambda)g}{3\epsilon(1+\lambda)^2}\frac{a_i}{E_0^2}, \tag{11}$$

$$Q_{V,ij} \equiv \frac{V_{ij}^{(0)}\dfrac{a_i+a_j}{2}}{\dfrac{D_{ij}^{(0)}}{kT}A} = \frac{2\pi\lambda(1-\lambda^2)|\rho_d - \rho_0|g}{3A}a_i^4, \tag{12}$$

where $Q_{V,ij}$ is proportional to a_i^4 and is very large compared with unity for typical dispersions (Zhang and Davis, 1991); therefore, the contribution of van der Waals forces to the relative motion of drops is small unless the drops are very close to one another. By contrast, $Q_{E,ij}$ depends primarily on the strength of the applied electric field and typically varies in the range from 10^{-2} to infinity.

The trajectory equation is integrated numerically along the drop trajectory from infinite separation of two drops to the point of their collision. Due to interactions between two drops, the drops move along curved trajectories, and a limiting trajectory occurs when the relative motion of the drops brings them to a point where contributions from the electric-field-induced force and van der Waals attraction just balance that from the gravitational force at $\theta \sim \pi$, as shown in Figure 6. From the limiting trajectory, the critical impact displacement, y_c, may be readily obtained, and then the collision efficiency calculated via Eq. 9. It is plain from the trajectory equation (Eq. 10) that the trajectories of two drops in relative motion, and the critical impact displacement or the collision efficiency, depend primarily on the balances of forces on the two drops, namely, the force parameters, $Q_{E,ij}$ and $Q_{V,ij}$.

Results

Of particular interest in the current study is the enhancement of drop collision and coalescence by an external electric field, whose strength relative to gravity is described by the parameter $Q_{E,ij}$. Therefore, in what follows calculated values of the collision efficiency, e_{ij}, are presented primarily as a function of $Q_{E,ij}$ while holding $Q_{V,ij}$ constant.

Figure 7 illustrates the effect of a horizontal electric field on drop collision, where the collision efficiency is plotted as a function of the parameter $Q_{E,ij}$ for different size ratios, λ, viscosity ratios, $\hat{\mu}$, and a typical value of the van der Waals attraction parameter of $Q_{V,ij} = 10^3$ (Zhang and Davis, 1991). As expected, the collision efficiency increases significantly as the strength of the electric field increases, or as $Q_{E,ij}$ decreases. When the electrostatic forces on the drops are sufficiently small compared to the gravitational forces on them, that is, $Q_{E,ij}$ is large, the collision efficiency asymptotically

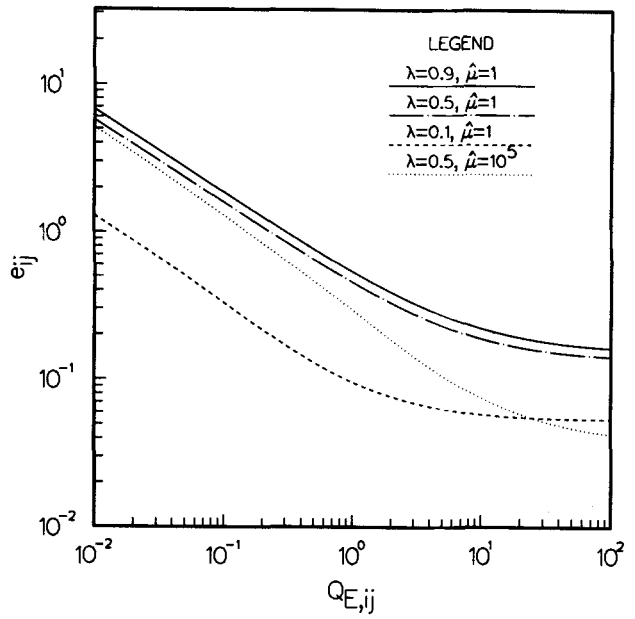

Figure 7. Collision efficiency, e_{ij}, as a function of electric-field-induced force parameter, $Q_{E,ij}$, in the presence of a horizontal electric field.

The variation of e_{ij} with $Q_{E,ij}$ is shown for different size ratios and viscosity ratios with the van der Waals force parameter $Q_{V,ij} = 10^3$.

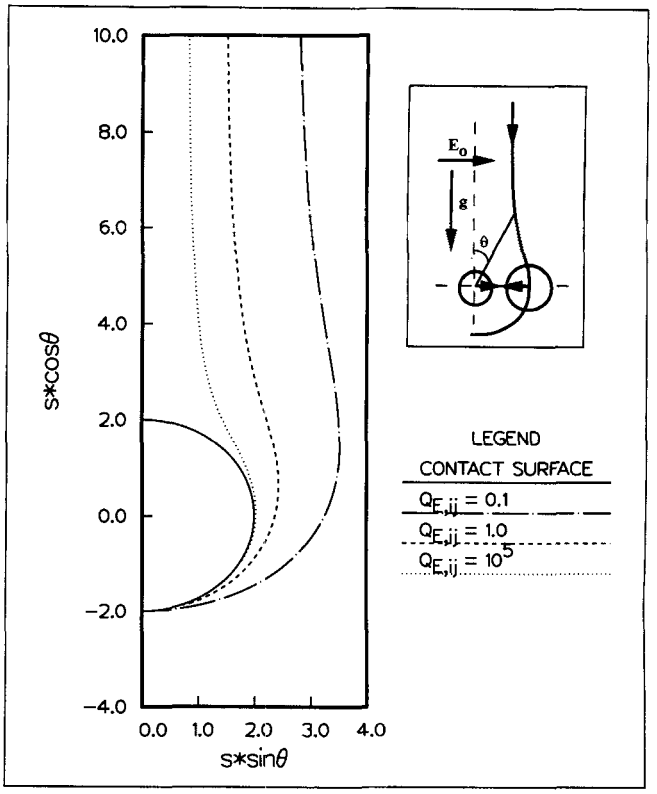

Figure 8. Limiting relative trajectories of two drops under a horizontal electric field.

$\lambda = 0.5$, $\hat{\mu} = 1$, $Q_{V,ij} = 10^3$, and different values of the electric-field-induced force parameter.

approaches that induced by gravity alone (Zhang and Davis, 1991). Figure 7 also shows that the collision efficiency decreases as the size ratio decreases. The latter occurs because (i) electric-field-induced forces decrease as the size ratio decreases, as shown in Figure 2, and (ii) the smaller drop tends to follow the streamlines of the flow and move around the larger one: hence collision does not occur unless the smaller drop is on a streamline that is very close to the larger drop. Moreover, Figure 7 demonstrates the effects of hydrodynamic interactions, which are characterized by the viscosity ratio, $\hat{\mu}$, on drop collision. As the viscosity of the drop phase increases, the resistance experienced by the drops in squeezing the fluid out of the gap separating them increases, resulting in a decrease in the possibility of collision of the two drops. Plainly, the influence of hydrodynamic interactions is especially pronounced when the electric-field-induced forces are small.

The enhancement of drop collision by an externally applied electric field can be perceived directly from the limiting relative trajectories of two drops, which are shown in Figure 8 for the situation in which $\lambda = 0.5$, $\hat{\mu} = 1$, $Q_{V,ij} = 10^3$, and different values of $Q_{E,ij}$. Two drops under a strong electric field experience a large electric-field-induced attraction and are pulled together rapidly, even when the initial value of the horizontal component of the separation between their centers is large, compared to those under the influence of a weak electric field, resulting in a large collision efficiency. The electrostatic force along the line of centers of the two drops, which acts directly to pull the drops into contact, rises as both their separation and the angle ψ fall (cf. Figures 2 and 4, respectively). The latter varies continuously as the drops move around each other and the angle θ increases (note that under a horizontal electric field, $\psi = |\theta - \pi/2|$, as shown in Figure 8). Therefore, the two drops experience the largest electric-field-induced attraction when they are aligned horizontally, which causes them to approach each other each other rapidly.

By contrast to a horizontal field, the effect of a vertical electric field on drop collision and coalescence is more complex. Moreover, the collision efficiency of the drops in a vertical field is found to be about one order of magnitude smaller than that in a horizontal field under otherwise the same conditions. This discovery is shown quantitatively in Figure 9 in the situation of $\hat{\mu} = 1$, $Q_{V,ij} = 10^3$, and different values of λ. The drastic change in the collision efficiency due to the orientation of the electric field can be clarified with the aid of Figure 10, which shows the limiting relative trajectories of two drops in relative motion for different values of the parameter, $Q_{E,ij}$, when the electric field acts vertically. As in the previous case of drop collision under a horizontal electric field, two drops that are initially widely separated approach one another, driven primarily by gravity. As the drops approach one another, hydrodynamic interactions cause them to flow around each other, which results in increases in the angles θ and ψ ($\psi = \theta$ in a vertical electric field), as shown in Figure 10. When the drops are aligned nearly horizontally, that is, $\psi \sim \pi/2$, the repulsion between the induced charges on the two drop surfaces pushes them apart (cf. Figure 4): therefore, the two drops cannot collide unless they start initially from a very small horizontal displacement, leading to a small collision efficiency. As mentioned earlier, because the

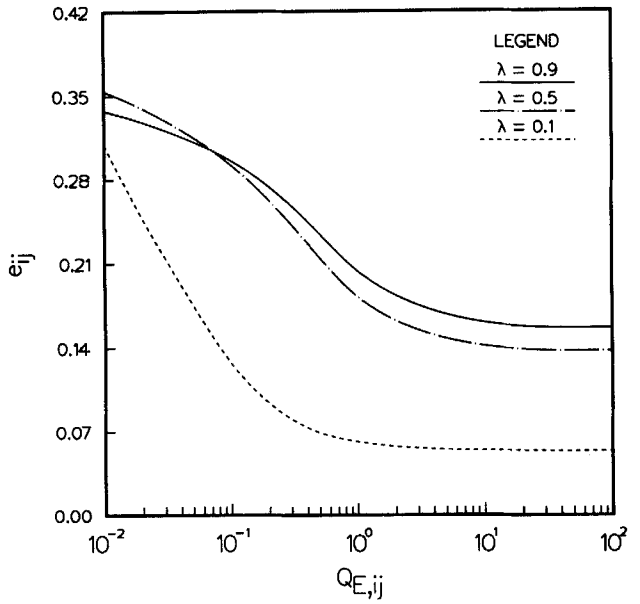

Figure 9. Collision efficiency, e_{ij}, as a function of electric-field-induced force parameter, $Q_{E,ij}$ in the presence of a vertical electric field.

The variation of e_{ij} with $Q_{E,ij}$ is shown for different size ratios with viscosity ratio $\hat{\mu} = 1$ and van der Waals force parameter $Q_{V,ij} = 10^3$.

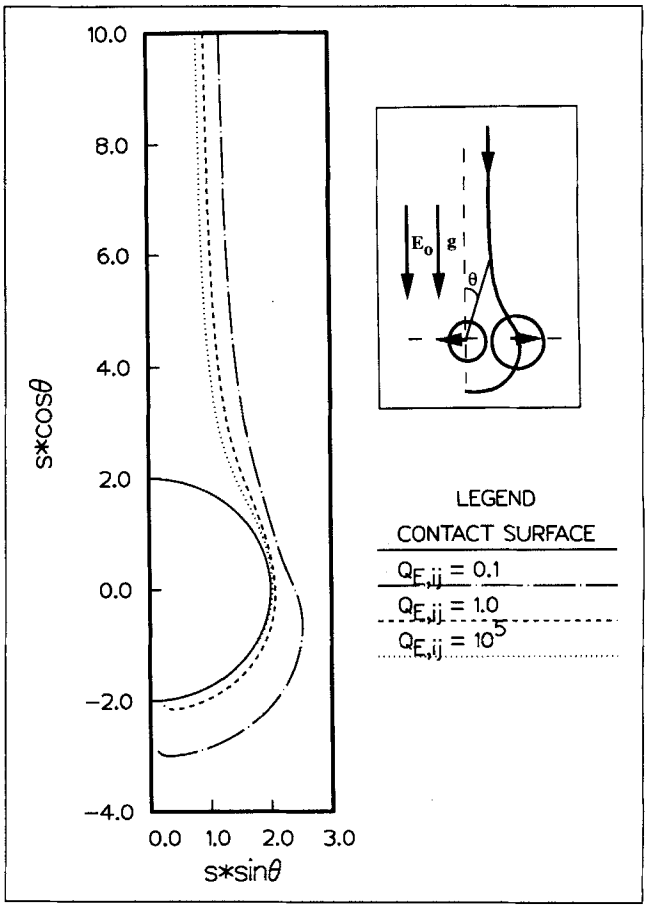

Figure 10. Limiting relative trajectories of two drops under a vertical electric field.

$\lambda = 0.5$, $\hat{\mu} = 1$, $Q_{V,ij} = 10^3$, and different values of the electric-field-induced force parameter.

electrostatic force on two drops increases as the drop-size ratio increases, so does the repulsion between them when $\psi \sim \pi/2$. Figure 9 shows that the stronger repulsion experienced by drops having large size ratios results in the collision efficiency of drops having $\lambda = 0.9$ to be smaller than that of drops having $\lambda = 0.5$ when the electric field is large enough, or $Q_{E,ij}$ is small enough.

Even though the *collision efficiency* in general increases as the size ratio increases, as shown in Figures 7 and 9, Figure 11 shows that the *collision rate* attains a maximum at moderate values of the size ratio for a typical situation where the drop and continuous phases viscosities are equal (that is, $\hat{\mu} = 1$) and the electric field acts horizontally. Here, the collision rate is nondimensionalized with a quantity not involving the size ratio: $J_{ij}/(n_i n_j \pi a_i^2 U_i^{(0)}) = e_{ij}(1-\lambda^2)(1+\lambda)^2$. The collision rate goes to zero in the limit of $\lambda = 0$ because of the vanishing collision efficiency, as discussed earlier, and also in the limit of $\lambda = 1$ because of the vanishing of the relative velocity of two widely separated drops, $V_{ij}^{(0)}$ (cf. Eq. 2). The variation of the dimensionless collision rate with the size ratio of two drops under a vertical electric field is qualitatively similar to that of two drops in a horizontal electric field (not shown). Moreover, as expected, the values of the dimensionless collision rate are greatly reduced in the former case compared to the latter one.

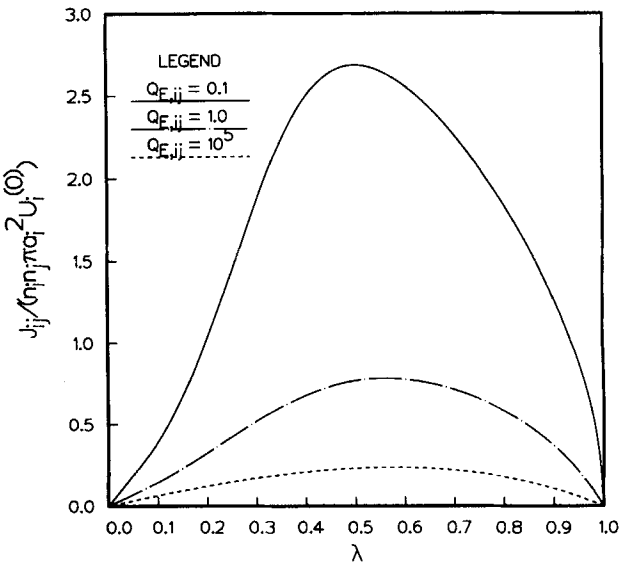

Figure 11. Dimensionless collision rate, $J_{ij}/(n_i n_j \pi a_i^2 U_i^{(0)}) = (1-\lambda^2)(1+\lambda^2)e_{ij}$, for drops under a horizontal electric field as a function of the size ratio when $\hat{\mu} = 1$, $Q_{V,ij} = 10^3$, and various values of $Q_{E,ij}$.

Collision Rate and Drop Growth in a Model Water–Oil Dispersion

Predictions of drop growth due to gravitational and electrostatic forces were made for a typical hydrosol dispersion, water drops in an oil, which is widely used in studies on electrocoalescence (Williams and Bailey, 1986; Ptasinski and

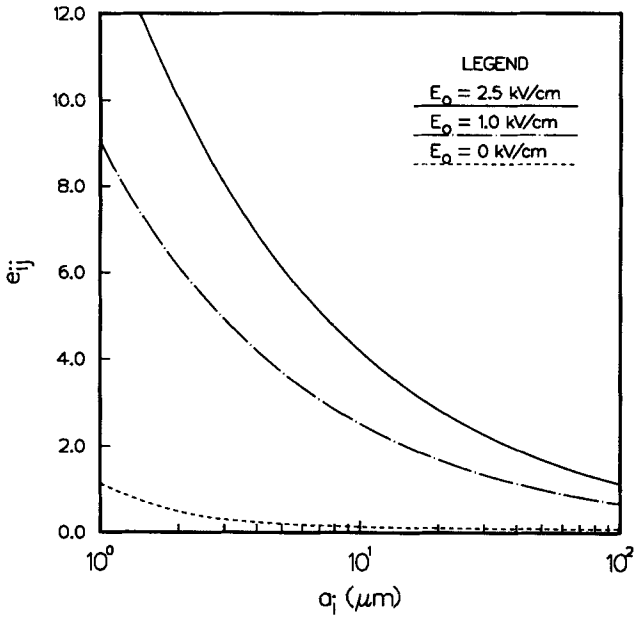

Figure 12. Collision efficiency for two water drops in an oil under a horizontal electric field as a function of the radius of the larger drop for $\lambda = 0.5$ and various electric field strengths.

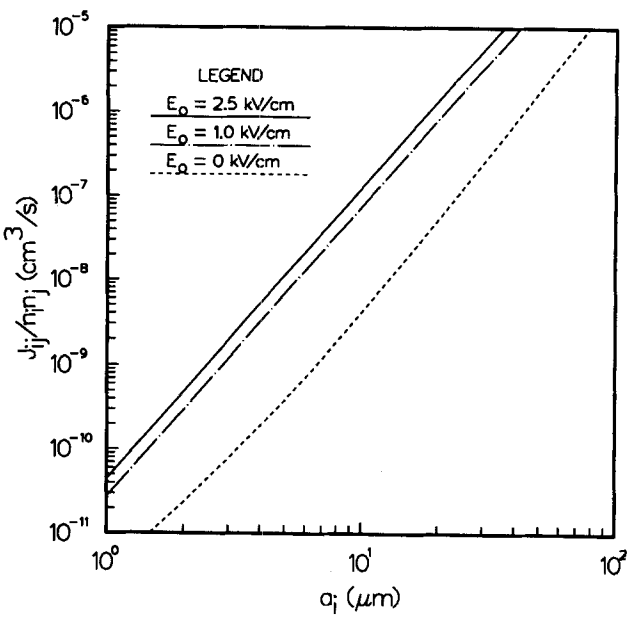

Figure 13. Collision rate for two water drops in an oil under a horizontal electric field as a function of the radius of the larger drop for $\lambda = 0.5$ and various electric field strengths.

Kerkhof, 1992), in order to gain a better understanding of the drop collision and growth processes. The relevant properties of this system are $\mu_0 = 0.0082$ g/cm·s, $\hat{\mu} = 1.22$, $|\rho_0 - \rho_d| = 0.18$ g/cm^3, and $\epsilon = 2.3$ (cf. Williams and Bailey, 1986). The Hamaker constant is estimated to be $A = 2.4 \times 10^{-13}$ erg (Hiemenz, 1986). Using these values in Eqs. 11 and 12 yields

$$Q_{E,ij} = 0.1285 \frac{\lambda(1-\lambda)}{(1+\lambda)^2} \frac{a_i}{E_0}, \tag{13}$$

and

$$Q_{V,ij} = 0.1539\lambda(1-\lambda^2)a_i^4, \tag{14}$$

where a_i is in microns and E_0 is in statvolt/cm. For this model system, attention is focused here on enhancement of drop coalescence by a horizontal electric field. Figure 12 shows the collision efficiency for this system as a function of the size of the larger drop, a_i, with $\lambda = 0.5$ and for various electric field strengths, E_0. Again, the collision efficiency is found to rise as the strength of the electric field rises. Moreover, the collision efficiency is larger for smaller drops compared to larger ones due to the increased importance of the attractive electric-field-induced forces and van der Waals forces relative to gravitational forces, that is, due to decreasing $Q_{E,ij}$ and $Q_{V,ij}$. Figure 13 shows similar results where the collision rate has been divided by $n_i n_j$. In addition to increasing with rising electric field strength, the collision rate increases significantly, although the collision efficiency decreases, as drop size rises, a result that accords with the definition of the collision rate at Eq. 2.

The growth of a population of water drops in a homogeneous, isotropic dispersion was studied by solving the population balance equation, Eq. 1, using the method developed by Berry and Reinhardt (1974). The earlier calculated results for the collision rate, part of which are shown in Figure 13, were used to compute the evolution of a population of drops. Figure 14 shows the evolution in time of the drop-size distribution for a system with a volume fraction $\phi = 0.1\%$ under a horizontal electric field of $E_0 = 2.5$ kV/cm. The initial size distribution was chosen to be a normal distribution with a

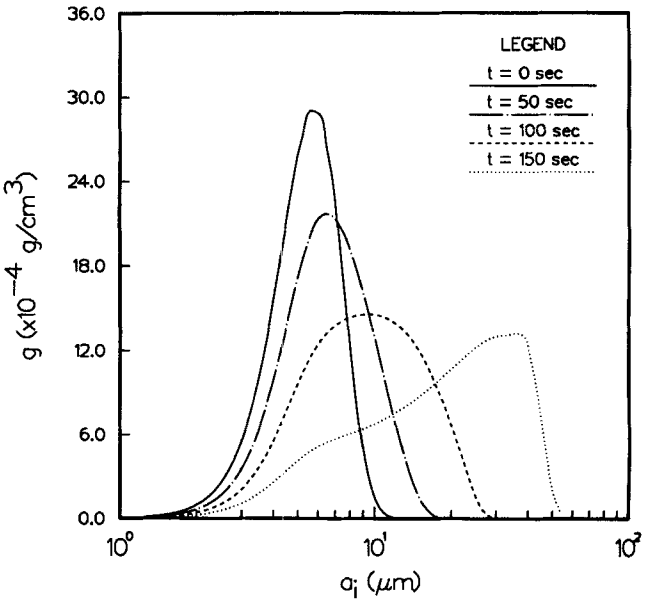

Figure 14. Evolution in time of the drop-size distribution in a water–oil dispersion under a horizontal electric field with $E_0 = 2.5$ kV/cm.

The initial size distribution, shown by the solid line, is a normal distribution.

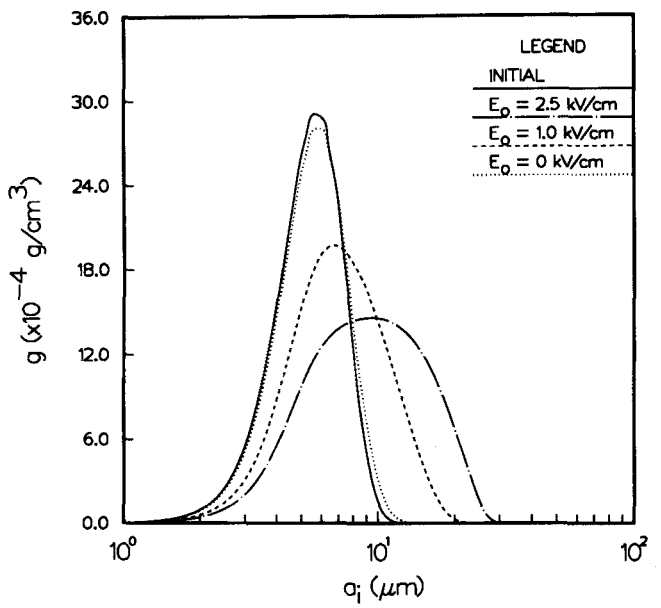

Figure 15. Drop-size distributions in water–oil dispersions under horizontal electric fields of different field strengths after 100 s.

In each case, the initial size distribution, shown by the solid line, is the same normal distribution.

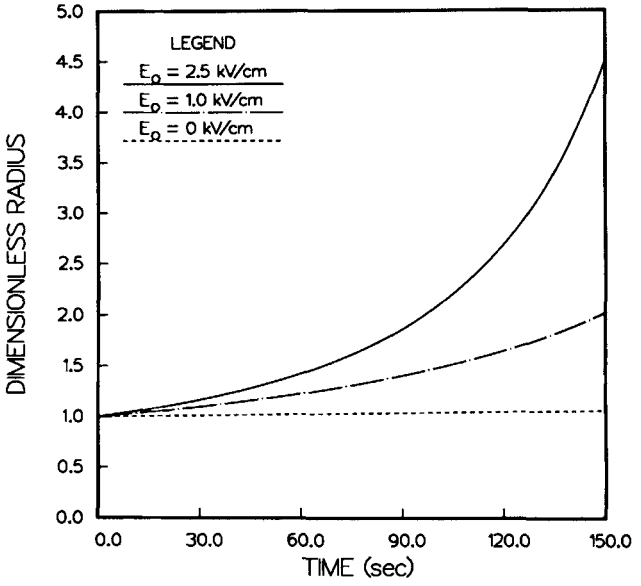

Figure 16. Evolution in time of mass-average drop radius, nondimensionalized by the initial radius, for a water–oil dispersion under horizontal electric fields of different strengths.

number-average radius of 3 μm and standard deviation of 2 μm and was discretized into size categories for which the drop mass doubles every fourth category. The function g plotted in Figure 14 is defined such that (Rogers and Davis, 1990)

$$\int_0^\infty g(\ln a)d\ln a = \phi. \tag{15}$$

Figure 14 shows that due to the enhanced coalescence of water drops under an electric field, the initial peak of the size distribution gives way to a second peak that rapidly shifts toward larger sizes after a period of drop coalescence. The larger spread in the evolved drop-size distribution is due to the combined effects of the stronger dependence of the collision rate on the size and size ratio. In other words, drop growth is dominated by collisions between drops of large sizes and moderate size ratios, as discussed earlier. The features of this spread in evolved drop-size distributions have also been found by Wang and Davis (1993) for drop coalescence due to gravity or thermocapillary effects.

The enhancement of drop growth by the applied electric field is clearly presented in Figure 15, which shows drop-size distributions that result after 100 s of drop coalescence in dispersions subjected to different electric fields of different strengths. Figure 16 shows the drop growth in this system in terms of the variation of the mass averaged drop radius, normalized by its initial value, as a function of time. As expected, the predicted results demonstrate a significant increase in drop size and a large shift in the drop-size distribution toward the large size, as the strength of an externally applied horizontal electric field increases. The latter result further reinforces the role played by an external electric field in enhancement of drop growth.

Concluding Remarks

Detailed quantitative predictions of collision and coalescence rates of two conducting, spherical drops and growth of a population of such drops induced by combined gravitational and electric-field-induced forces are presented in this article for the first time. By using a trajectory analysis to follow the relative motion of pairs of drops and completely accounting for hydrodynamic and electrostatic interactions between the drops, predictions are made of the rate of pairwise drop collisions. A dynamic population balance equation is then solved to determine the evolutions in time of the drop-size distribution and the average drop size in a dilute water–oil dispersion due to drop coalescence. The results show that the collision rate and the drop growth increase significantly by imposing an external electric field. The enhancement of drop collision and coalescence is especially pronounced when the imposed electric field acts horizontally. Moreover, the results show that the increase in the rates of drop collision and coalescence are larger for larger drops over smaller ones, which leads to a large spread in the resultant drop-size distribution.

The model presented here may be used to predict collision and coalescence of conducting, spherical drops under different processing conditions, namely varying strengths and orientations of the imposed electric field, properties of the liquid–liquid system, and the relative geometry of drops. The method can also be extended to more complicated cases. For example, collision and coalescence of drops bearing net charge under an electric field can be readily studied by a straightforward extension of the analyses of this article. This would amount to solving the Laplace equation that governs the distribution of electric field or potential outside the conducting drops subject to charge constraints (cf. Basaran and Scriven, 1989). Furthermore, the drops and the surrounding fluid need not be perfect conductors and perfect insulators,

respectively, but could be so-called semi-insulators or leaky dielectrics (Taylor, 1966; Melcher and Taylor, 1969). In this case, however, the mathematical problem to be solved is much more complicated than the one considered in this article (cf. Basaran and Scriven, 1988). This is because, whereas the flow and electric field problems are uncoupled in this article, they are coupled and must be solved simultaneously when both the dispersed and the continuous phases are endowed with finite conductivities. Substantial extensions of the present model to render it capable of handling the more complicated situation involving leaky dielectrics and experiments to study drop collision and coalescence under gravity and an electric field are ongoing research projects in our laboratory.

Acknowledgments

This work was supported by the Division of Chemical Sciences, Office of Basic Energy Sciences, U.S. Department of Energy, under Contract DE-AC05-84OR21400 with Martin Marietta Energy Systems, Inc. The authors thank Professor R. H. Davis for providing certain details of his calculations.

Literature Cited

Allan, R. S., and S. G. Mason, "Particle Motion in Sheared Suspensions," *J. Colloid Sci.*, **7**, 383 (1962).

Basaran, O. A., and L. E. Scriven, "The Taylor Pump: Viscous-Free Surface Flow Driven by Electric Shear Stress," *Chem. Eng. Commun.*, **67**, 259 (1988).

Basaran, O. A., and L. E. Scriven, "Axisymmetric Shapes and Stability of Charged Drops in an External Electric Field," *Phys. Fluids*, **A1**, 799 (1989).

Batchelor, G. K., "Sedimentation in a Dilute Polydisperse System of Interacting Spheres," *J. Fluid Mech.*, **119**, 379 (1982).

Berry, E. X., and R. L. Reinhardt, "An Analysis of Cloud Drop Growth by Collection: Part I. Double Distributions," *J. Atmos. Sci.*, **31**, 1814 (1974).

Davis, M. H., "Two Charged Spherical Conductors in a Uniform Electric Field: Forces and Field Strength," *Quart. J. Mech. Appl. Math.*, **17**, 499 (1964).

Haber, S., G. Hetsroni, and A. Solan, "On the Low Reynolds Number Motion of Two Droplets," *Int. J. Multiphase Flow*, **A1**, 57 (1973).

Hadamard, J. S., "Mouvement Permenent Lent d'Une Sphere Liquide et Visqueuse Dans un Liquide Visqueux," *C. R. Acad. Sci. (Paris)*, **152**, 1735 (1911).

Hamaker, H. C., "The London-van der Waals Attraction Between Spherical Particles," *Physica*, **4**, 1058 (1937).

Hiemenz, P. C., *Principles of Colloid and Surface Chemistry*, Marcel Dekker, New York/Basel (1986).

Kim, S., and S. J. Karrila, *Microhydrodynamics: Principles and Selected Applications*, Butterworth-Heinemann, Boston (1991).

Landau, L. D., and E. M. Lifshitz, *Electrodynamics of Continuous Media*, Pergamon, New York (1960).

Latham, J., and I. W. Roxburgh, "Disintegration of Pairs of Water Drops in an Electric Field," *Proc. R. Soc. Lond.*, **A295**, 84 (1966).

Melcher, J. R., and G. I. Taylor, "Electrohydrodynamics: A Review of the Role of Interfacial Shear Stresses," *Ann. Rev. Fluid Mech.*, **1**, 111 (1969).

Michael, D. H., and M. E. O'Neil, "Electrohydrodynamic Instability in Plane Layers of Fluid," *J. Fluid Mech.*, **41**, 571 (1970).

Ptasinski, K. J., and P. J. A. M. Kerkhof, "Electric Field Driven Separations: Phenomena and Applications," *Sep. Sci. Technol.*, **27**, 995 (1992).

Rogers, J. R., and R. H. Davis, "The Influence of van der Waals Attractions on Cloud Droplet Growth by Coalescence," *J. Atmos. Sci.*, **47**, 1057 (1990).

Rybczynski, W., "Uber die Fortschreitende Bewegung Einer Flussigen Kugel in Einem Zahen Medium," *Bull. Acad. Sci. Cracovie*, **A**, 40 (1911).

Sartor, J. D., "Electricity and Rain," *Phys. Today*, **22**, 45 (1969).

Satrape, J. V., "Interactions and Collisions of Bubbles in Thermocapillary Motion," *Phys. Fluids*, **A4**, 1883 (1992).

Taylor, G. I., "Studies in Electrohydrodynamics. I. The Circulation Produced in a Drop by an Electric Field," *Proc. R. Soc. Lond.*, **A291**, 159 (1966).

Tien, C., and A. C. Payatakes, "Advances in Deep Bed Filtration," *AIChE J.*, **25**, 737 (1979).

Wang, H., and R. H. Davis, "Droplet Growth due to Brownian, Gravitational, or Thermocapillary Motion and Coalescence in Dilute Dispersions," *J. Colloid Interface Sci.*, **159**, 108 (1993).

Waterman, L. C., "Electrical Coalescers," *Chem. Eng. Prog.*, **61**, 51 (1965).

Williams, T. J., and A. G. Bailey, "The Resolution of Water-in-Oil Emulsion Subjected to External Electric Fields," *Inst. Phys. Conf. Ser.*, **66-II**, 39 (1983).

Williams, T. J., and A. G. Bailey, "Changes in the Size Distribution of a Water-in-Oil Emulsion Due to Electric Field Induced Coalescence," *IEEE Trans. Ind. Appl.*, **IA-22**, 536 (1986).

Zhang, X., and R. H. Davis, "The Rate of Collisions of Small Drops Due to Brownian and Gravitational Motion," *J. Fluid Mech.*, **230**, 479 (1991).

Zhang, X., and R. H. Davis, "The Collision Rate of Small Drops Undergoing Thermocapillary Migration," *J. Colloid Interf. Sci.*, **152**, 548 (1992).

Zinchenko, A. Z., "The Slow Asymmetric Motion of Two Drops in a Viscous Medium," *Prikl. Mat. Mech.*, **44**, 30 (1981).

Manuscript received July 11, 1994, and revision received Sept. 12, 1994.